AGH Journal of Mining and Geoengineering • Vol. 36 • No. 2 • 2012

*Janusz Ukleja *, Damian Bęben *, Wojciech Anigacz **

DETERMINATION OF THE RAILWAY RETAINING WALL DIMENSIONS AND ITS FOUNDATION IN DIFFICULT TERRAIN AND UTILITY

1. Introduction

The subject of the paper is the analysis of the retaining wall laid on unknown ground. The paper demonstrates how to determine the geometry of the wall and its foundations, as well as the course and extent of substrate rock. The GPR technique and test excavations were used to achieve the objectives. Field tests involved scanning the ground near the railway tracks, the retaining wall and its base.

Ground Penetrating Radar (GPR) is a high resolution electromagnetic (EM) technique. This method is designed for non-destructive investigations of the deep and shallow subsurface of the soil, structural elements, roads and bridges. The fundamental principles and theory of GPR operation have evolved for many years. It results from the development of electrical engineering, geophysical and seismic testing [1].

However, there are some limitations with this method when used for the determination of and distinguishing individual layers of the ground. Therefore, an additional system of open pits nearby and partly within the study area were applied. Taking into account the nature of the ground (the rock of soft shales, in the form of the rock, debris and waste), found in the vicinity of the retaining wall, execution of the pits as a calibration of the GPR technique gave very clear and reliable results.

2. Description of the structure and its technical condition

The retaining wall was built in 1912. The load-bearing system of the wall constitutes a massive stone structure on lime mortar. Its average thicknesses is about 0.90–1.05 m.

* Opole University of Technology, Faculty of Civil Engineering, Opole

The retaining wall consists of two parts, the first has a length of about 6.0 m and height of 4.0 m (Fig. 1a). The length of the second part amounts to 135 m, and the height is variable, i.e. from 1.5 m (on ends of the wall) to 7.5 m (in the middle part) counting from the level area (Fig. 1b). The securing of the railway embankment to the railway line is main task of the retaining wall. In the immediate vicinity of the wall is the river. The retaining wall in the plan has a shape of gentle arc which is parallel to railway track lines.

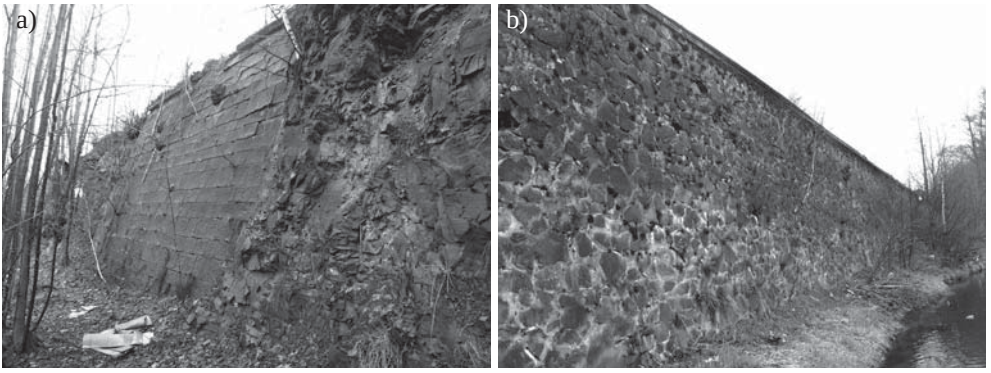

Fig. 1. The general side view of the retaining wall: a) part I, b), part II

The technical condition of the retaining wall aroused serious reservations and required immediate repair works. The upper part of the wall (up to about ⅓ of height), the bulges and the numerous gaps in joints between the individual stones had appeared. In the second part of the wall, numerous losses of the stone, both in of bottom and of top were observed. In the predominant parts of the wall there were no joints since they have been washed away by water. The local bulges in the wall and detached stone surface were visible in numerous places (Fig. 2a). The caverns in the wall resulting from washout of the mortar from the stones and this was observed in many places (Fig. 2b). Trees and bushes growing out of the wall increases its destruction. Although the visual technical condition of the stone elements had been determined as quite good, it has also been observed in many cases loose stones (without joints) which could potentially fall out of the wall. Lack of insulation and drainage as well as water flowing down on the wall elements and flushing out the joints has also had an effect on the destruction of the wall. Water also penetrated the embankment and flushed through the joints on the inside wall (especially during high tide in the river).

3. Description of the applied measurement technology and equipment

RIS Hi-MOD and RIS ONE type georadars were used in the field tests. The GPR technique involves the propagation of short EM pulses ($t \leq 1$ ns $= 10^{-9}$ s) in the medium being tested. The pulses are reflected in varying sharp changes in the EM properties of the medium, including the magnetic permittivity, electric conductivity and dielectric permittivity. These changes are related, for example, to the presence of heterogeneities inside the medium,

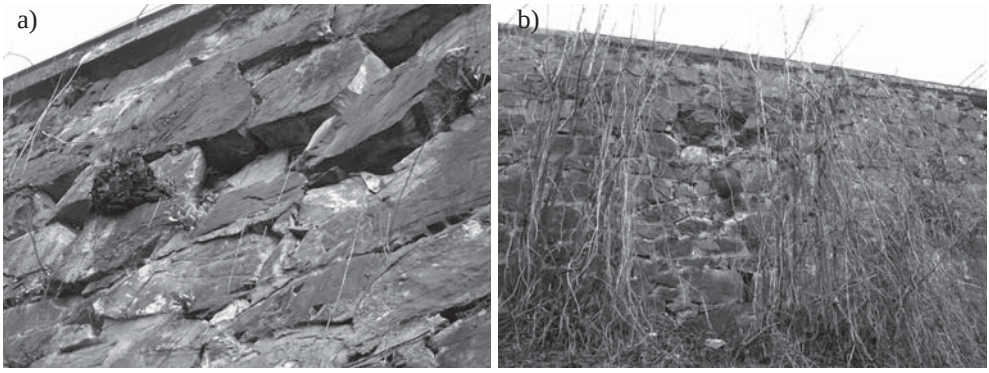

Fig. 2. Damages to the retaining wall: a) leach the mortar, b) visible the cavern

changes in the materials (such as the shallow geological layers) or changes in the physical properties of the medium (e.g. in the water content). To correctly interpret the GPR results (radargrams) it is necessary to compare the emitted waves with the recorded waves. The differences between them depend on the EM properties of the medium. The velocity of the wave is a characteristic of the signal, and is highly dependent on these EM properties. It also refers to the amplitude of the reflected wave and its frequency [2].

The result of the GPR (antenna) approaching an object (element), where the discontinuity medium, the distance d_{-n}, d_{-1}, etc. is decreasing (Fig. 3). Thus, the return time of the reflected wave from the object (element) to the receiver also decreases. From the combination of points giving information on distance (time) from an object at various points x_n, x_{-1}, etc., the hyperbole is created, which is a reflection of the object on the radargram (Fig. 3).

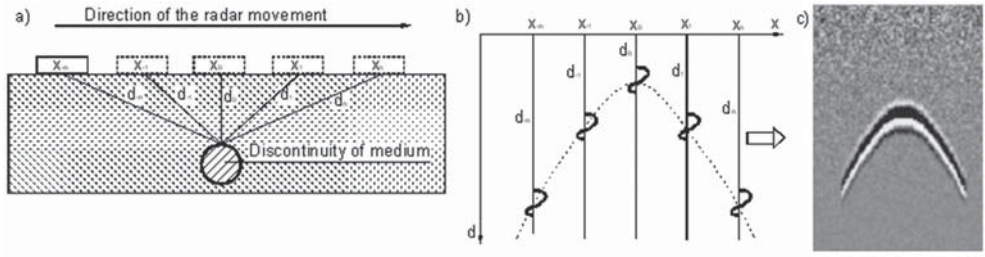

Fig. 3. Scheme presenting the general rule of operation GPR: a) measurement, b) graphical interpretation of the measurement, c) final map GPR

From a theoretical point of view, the GPR signal, $f(k)$, passing through an object (element) consisting of several layers can be analyzed as the sum of scaled and time-delayed replicas given by the incident signal $x(k)$, as shown by the following Eq. (1):

$$f(k) = \sum_{i=1}^{n} A_i \cdot x \cdot (k - t_i) + n(k) \tag{1}$$

where A_i is an attenuation factor, t_i is the time delay, and $n(k)$ is the added noise. The factors A_i and t_i depend mainly on the dielectric properties of the materials and the layer thicknesses [3].

The normalized root-mean-square error between the original GPR signal, $f(k)$, and the de-noised GPR signal, $r(k)$, can be calculated from the Eq. (2):

$$NRMSE = \sqrt{\frac{\overline{(f(k) - r(k))^2}}{(f(k) - u_f)^2}} \tag{2}$$

where μ_f is the mean value of the GPR signal $f(_k)$.

With penetration depth, vertical and horizontal resolution are the main limitations of the GPR method applications. Penetration depth is defined as a depth achieved when the amplitude has been attenuated by a factor e^{-1}. It indicates the capability of the radar signal to penetrate into the studied medium. It mainly depends on the attenuation factor and on EM wave changes. The horizontal resolution indicates the capability of the GPR system to detect two different elements in the direction of the antenna movement. From a practical point of view, it is shown as two different anomalies in the GPR record. It depends on the antenna frequency, the penetration depth and the EM properties of the tested medium. In turn, the vertical resolution or so-called resolution in time, is defined as the capability of the antenna to detect two hozontal discontinuities as separate anomalies. This parameter also depends on wave velocity and its length [4].

The reflection of the emitted energy (the EM wave) occurs in intense changes of the dielectric parameters. The reflection coefficient is strictly related to the dielectric constants of the given material (element). This coefficient determines the part of the incident wave that is reflected. The sum of these coefficients (transmission and reflection) is equal to one. So, the following relationship can be introduced (3) [2]:

$$R = \frac{\sqrt{\varepsilon_{r1}} - \sqrt{\varepsilon_{r2}}}{\sqrt{\varepsilon_{r1}} + \sqrt{\varepsilon_{r2}}} \tag{3}$$

where ε_{r1} and ε_{r2} are the relative permittivity of the upper and lower layer of element, respectively. The relationship (3) clearly indicates that the size of the reflected wave at the interface between two media depends on the size of the dielectric constant.

The georadars used in the study had different operating frequencies, i.e., RIS Hi-MOD (the dual frequency of 200/600 MHz, i.e., it has the opportunity during one passage of GPR to perform two scans with different frequencies) and RIS ONE (80 MHz).

The area track was examined using three longitudinal (L) and three transverse (T) scans. Longitudinal scans were determined between: (i) south rail track and the edge of the retaining wall (L1 scan), (ii) railway track lines (L2 scan), and (iii) north rail track and the slope along the outcrop of rocks (L3 scan). Scans were carried out from east to west. However the transverse scans (T1–T3) were conducted from the slope towards the edge of the wall (to the south) at right angles to the outcrop of rocks in the slope (Fig. 4).

The retaining wall was examined using four scans: two on the east and two on the west side. Scanning of the wall was performed at the height of about 1.50 m from ground level. Moreover, scanning of the river (right on the edge of the wall) was also conducted. The scan "Bank_L1" began at the end of the scan "Wall_L2" and ran in the opposite direction. The scan "Bank_L2" constitutes his continuation. Scans "Wall_L3" and "Bank_L3" were performed on the west side of the wall.

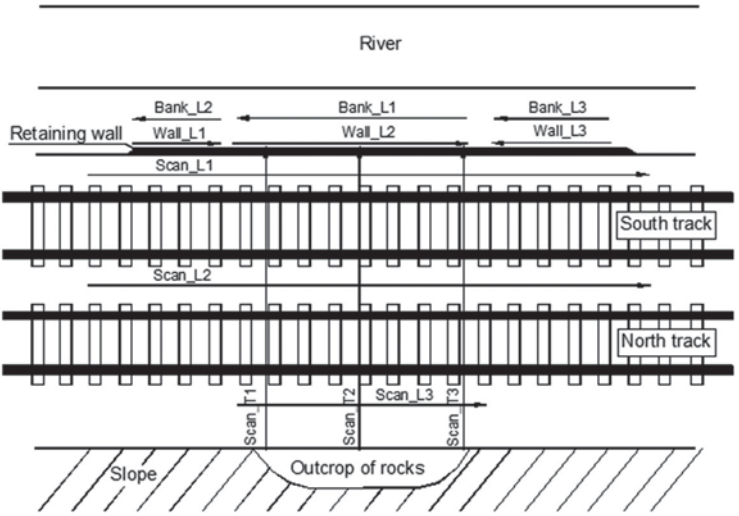

Fig. 4. The scheme of arrangement of the longitudinal (L) and transverse (T) scans

4. The results of the tests and their analysis

The results obtained by the GPR test were processed using GRED 3D Utilities software. Data processing was conducted using the proper filters and signal gains. All GPR results were processed by the following filters:

1) Move start time — filter moving all scanning results to 0 level.
2) Background removal — filter removing the unnecessary background (disturbances) in the form of horizontal lines.
3) Vertical bandpass filter (TD) — sliding filter for selected frequencies (for the antenna of 80 MHz: from 50 to 150 MHz; for the antenna of 200 MHz: from 100 to 300 MHz and for the antenna of 600 MHz: from 400 to 800 MHz).
4) Linear gain — improving the quality of the displayed results.
5) Smoothed gain — improving radargram sharpness.

4.1. Trackway

The area of the trackway was tested using both the available GPR (RIS Hi-MOD and RIS-ONE) along the same routes. However, because of the need to set the bedding of the

wall, the authors in this paper only focused on the presentation and the analysis of the results for the antenna of 80 MHz, which allows one to perform the scan at greater depth.

Fig. 5a–c presents selected radargrams for longitudinal scans (L). On 14 m of the radargram, at a depth of 1.2 m a disorder starts — probably at the beginning of the retaining wall (Fig. 5a). At a depth of about 1.6 m (from 1.5 to maximum 1.9 m) the layer of the ground is clearly visible. Additionally, three large anomalies are visible at a depth of the about 2 m at the beginning of the scan, on 59 m and on 115 m, what constitutes a reflection from the external objects. As it turned out, these were the anchors used during earlier repairs to stabilize the retaining wall. On the outer wall texture there are visible balls, representing the heads of anchors.

In figure 5b the same three large anomalies are shown at a depth of about 2 m located at the beginning of the scan, i.e. at 0 m, 59 and 115 m — probably a reflection from the external

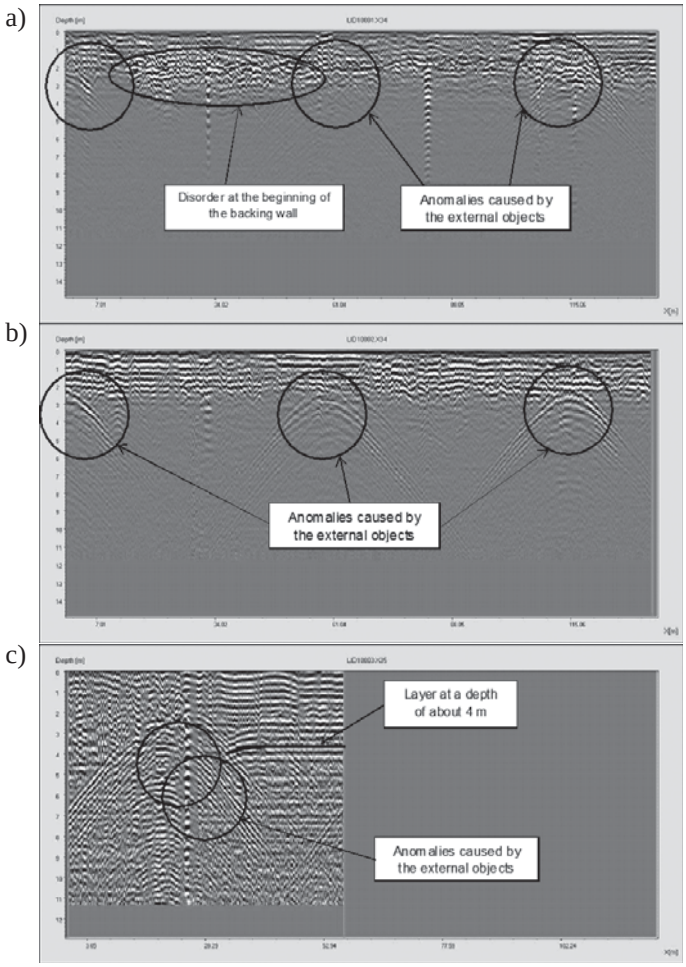

Fig. 5. GPR maps for scans: a) L1 (nearby the wall), b) L2 (between the rail tracks), c) L3 (nearby the slope)

objects. There were no other anomalies and track substructure layers were evenly placed to a depth of 2.5–3.0 m.

Figure 5c presents the fragment of a layer at a depth of 4 m — it is likely that it is a layer of rock. As before, two large anomalies were noted at 17 and 25 m of the scan.

Figure 6a–c presents the maps of GPR for the transverse scans conducted perpendicular to the retaining wall (T). Fig. 6a presents the layer of about 3.5 to 3.0 m (red line) — the likely limit of the trackbed. The green line determines the layer extending from a depth of 3.5 m down — this is a layer of rock. A similar course, trackbed and bedrock layers were observed in figure 6b–c.

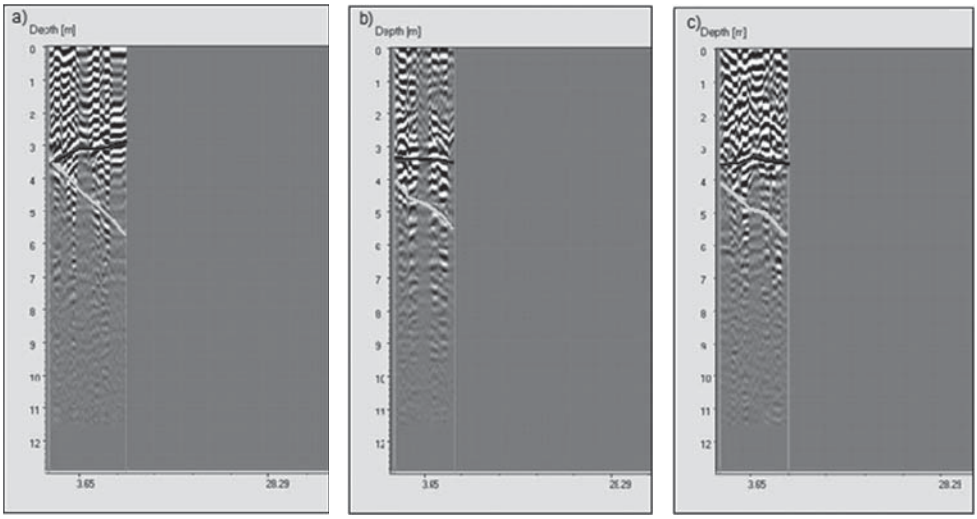

Fig. 6. Fragments of GPR maps for transverse scans: a) T1, b) T2 and c) T3

4.2. Tests of wall and the river bank

The GPR RIS Hi-MOD stocked in the antenna with dual operating frequencies of 200/600 MHz was used to test the river bank. To determine the depth occurring of rocks in the primer base (by the river) was the main aim of profiling. Taking into account of the terrain conditions and the availability of the tested area, the antenna with a frequency of 80 MHz was not possible to application.

Fig. 7 a–b presents the radargrams for the longitudinal scan "Bank_L1", which were made using two frequencies of 200 and 600 MHz. The length of this scan was about 30 m and was situated in the middle part of the wall. In this figure, two layers are visible: one only fragmentary at depth of 0.20 m at endings to 0.60 m in the middle of the profile. The second layer is clearly descending down from the beginning of the profile with a depth of about 0.7 m to 1.4 m. The second layer is probably a layer of rocks near the wall. Other scans on "Bank_L2" and "Bank_L3" present similar results. The subsequent execution pits at the base of the wall confirmed the result obtained from the GPR testing.

Fig. 8 shows the radargram illustrating the thickness of the retaining wall at the height of approximately 1.5 m from the level of the terrain, which was made using an antenna with frequencies of 600 MHz. It is clear that the thickness of the retaining wall is about 1.0 m, and it also contains a number of free spaces (loss of stone) in the structure.

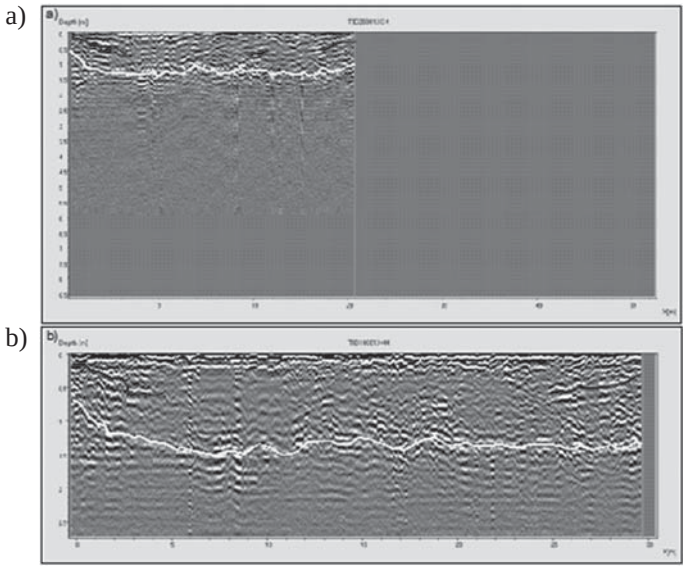

Fig. 7. GPR maps for the longitudinal scan "Bank_L1" made using antenna with frequencies: a) of 200 MHz and b) of 600 MHz

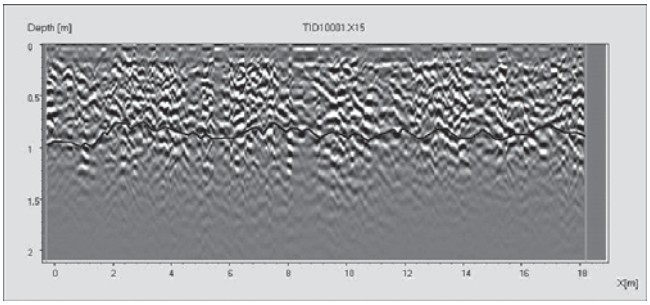

Fig. 8. Radargram of the retaining wall (longitudinal profile "Wall_L1") made using antenna with frequencies of 600 MHz

After analyzing the obtained GPR results, additional open pits were carried out in the form of excavation in the immediate vicinity of the retaining wall, situated in such a way as to correspond to the longitudinal (L) and transverse (T) scans of the GPR. Additionally, the inventory course of the outcrop of rock in the region of the retaining wall both from the slope side and the river, running at the base of the slope, were conducted. From the ground which takes up the space between the embankment slope and the retaining wall,

several samples were collected and subjected to the laboratory analysis. It was found that this is made up of fine debris rock slate loamy with the low humidity and the internal friction angle 45°. The rock waste passing into the solid rock loamy slate was found below the embankment.

Drawing lines of division of the layers obtained using GPR, from pits and rock outcrop observations led to the implementation of sections of retaining wall and rock layers. The most characteristic is presented in figure 9.

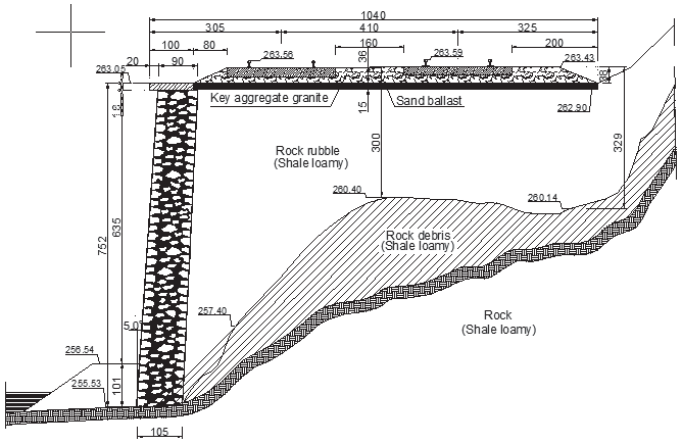

Fig. 9. Cross sections of the retaining wall and the rock layers

5. Summary

As a result of conducted tests on the terrain nearby the retaining wall using the GPR technique it was established, that:

1) The transverse and longitudinal scans of the trackway confirmed the following layers: appearing on depths ca. 1.5–3.0 m — which determined the lower limit of the trackbed, below a probable course of cracked rock appearing in the form of saportlite as well as the roof of the solid rock which steeply and consistently falls down to the depth over 5 m. The described course of the layers is confirmed in the open pits as well as in the outcrops of rocks nearby the retaining wall.
2) At a depth of the about 1.0–1.5 m from the level of the terrain under the foundation of the retaining wall, rock layers were found.
3) Shapes of parts of the wall were also determined. Its thickness at height of 1.5 m from ground level is about 1.0 m.
4) Additionally, on the length of the wall there several anomalies were located, i.e. reflections of the signal from elements behind the retaining wall. After analyzing all longitudinal scans, it was found that these reflections indicate the presence of anchors installed in the retaining wall during previous repair works.

5) The method applied proved effective and allowed basic data about the construction of the retaining wall and its foundations to be obtained. Difficult terrain conditions prevented the execution of complex geological-engineering testing in the traditional manner.

REFERENCES

[1] Bęben D., Mordak A., Anigacz W.: *Application of the GPR Technique for Determination of Bridge Beams Parameters.* Drogi i Mosty, vol. 10, no. 3, 2011, p. 5–22.

[2] Baili J., Lahouar S., Hergli M., Al-Qadi I.L., Besbes K.: *GPR Signal De-noising by Discrete Wavelet Transform*. NDT&E International, vol. 42, no. 8, 2009, p. 696-703.

[3] Daniels J.J.: *Ground Penetrating Radar Fundamentals.* Prepared as an appendix to a Report to the U.S.EPA, Region V. Nov. 25, 2000 (Ohio State University, Columbus, 2000), p. 1–21.

[4] Perez-Gracia V., Garcıa Garcıa F., Rodriguez Abad I.: *GPR Evaluation of the Damage Found in the Reinforced Concrete Base of a Block of Flats: A case study.* NDT&E International, vol. 41, no. 5, 2008, p. 341–353.